Longitudinal Changes to Tight Junction Expression and Endothelial Cell Integrity in a Mouse Model of Sterile Corneal Inflammation

Laura E. Downie, Janet Choi, Jeremiah K. H. Lim, and Holly R. Chinnery

Department of Optometry and Vision Sciences, Faculty of Medicine, Dentistry and Health Sciences, University of Melbourne, Parkville, Victoria, Australia

Correspondence: Holly R. Chinnery, Department of Optometry and Vision Sciences, University of Melbourne, Parkville, Victoria 3010, Australia;
holly.chinnery@unimelb.edu.au.

Submitted: December 22, 2015
Accepted: May 14, 2016

Citation: Downie LE, Choi J, Lim JKH, Chinnery HR. Longitudinal changes to tight junction expression and endothelial cell integrity in a mouse model of sterile corneal inflammation. *Invest Ophthalmol Vis Sci*. 2016;57:3477–3484. DOI:10.1167/iovs.15-19005

Purpose. We previously reported that applying toll-like receptor (TLR) ligands to an injured cornea induces corneal edema at 24 hours, which subsides by 1 week. We tested the hypotheses that endothelial expression of the tight-junction protein, zonula occludens-1 (ZO-1), would be altered during experimental sterile corneal inflammation and that endothelial cell density (ECD) would remain unaffected.

Methods. Anesthetized C57BL/6J mice received central 1-mm corneal abrasions followed by topical application of saline or cytosine-phosphate-guanosine oligodeoxynucleotide (CpG-ODN, TLR-9 agonist). At 24 hours, 1 week and 4 weeks post treatment, spectral-domain optical coherence tomography images were captured. Eyes were enucleated and processed for zonula occludens-1 (ZO-1) immunofluorescent staining. Corneal flatmounts were analyzed for endothelial ZO-1 expression, cell density, polymegethism, and polymorphism. Corneal stromal inflammatory cell infiltration was evaluated at 4 weeks by immunostaining for CD45.

Results. Central corneal thickness (CCT) was increased in CpG-ODN treated eyes at 24 hours, had normalized by 1 week, but was again thickened by 4 weeks. In eyes with CpG-ODN, endothelial cell ZO-1 expression was reduced at 24 hours but returned to normal levels by 1 week. Endothelial cell density was not altered at 24 hours or 1 week. By 4 weeks, only CpG-ODN eyes showed relatively reduced ECD, as well as large numbers of $CD45^+$ cells in the stroma. Changes to ECD correlated with CCT ($r = -0.53$, $P < 0.01$). Compared with naïve controls, more saline- and CpG-ODN–treated eyes exhibited polymegethism.

Conclusions. This study provides novel insights into the interplay between endothelial cell integrity, corneal edema, and chronic stromal leukocyte activation during sterile corneal inflammation in mice.

Keywords: inflammation, toll-like receptor, corneal endothelial cells

The integrity of the corneal endothelium is critical for the maintenance of stromal hydration and transparency. Injury or inflammation to this nonregenerative cell monolayer can have serious negative impacts upon corneal transparency and vision. Excluding corneal dystrophies, a range of inflammatory-mediated conditions, such as infectious keratitis,[1] anterior uveitis,[2] corneal graft rejection,[3] and dry eye disease[4] can affect the integrity of the corneal endothelium. Owing to the availability of noninvasive clinical imaging modalities, including slit lamp biomicroscopy and confocal laser scanning ophthalmoscopy,[5] the corneal endothelium can be readily visualized and monitored during the course of disease or inflammatory processes in humans and rodents. Furthermore, corneal endothelial integrity can be assessed indirectly by monitoring corneal edema in mice using spectral-domain optical coherence tomography (SD-OCT).[6]

Breakdown in endothelial tight junctions is associated with impaired ability of the cornea to control fluid uptake from the anterior chamber, leading to corneal edema and compromised light transmittance.[7] Epithelial stress, including hypoxia, is associated with aberrant expression of tight junctions between endothelial cells.[8] In studies of bovine endothelial cell cultures, exposure to the proinflammatory cytokine TNF-α causes a discontinuation of the apical endothelial tight junction protein zonula occludens-1 (ZO-1) and loss of transendothelial electrical resistance.[9] In similar studies, TNF-α–induced impairment of the endothelial tight junctions can be experimentally abrogated by inhibition of matrix metalloproteinase-9 (MMP-9).[10] In light of the ability of proinflammatory cytokines to affect tight junction expression in the corneal endothelium, we investigated the consequences of sterile, innate inflammation in the mouse cornea following topical application of the toll-like receptor (TLR)-9 agonist, cytosine-phosphate-guanosine (CpG)-DNA.

Application of TLR-9 ligand CpG-oligodeoxynucleotide (ODN) to the injured mouse cornea induces an acute phase of neutrophil and macrophage infiltration and corneal edema[6,11,12] followed by a later accumulation of giant macrophages in the stroma and keratic precipitates on the corneal endothelium.[13] The accumulation of keratic precipitates is not associated with overt structural changes to the corneal endothelium, and corneal edema largely subsides by 1 week,

Investigative Ophthalmology & Visual Science

suggesting that the presence of inflammatory cells in the cornea is not associated with corneal endothelial dysfunction. To explore the mechanisms of increased corneal edema during the acute phase of CpG-induced corneal inflammation, we investigated the expression of the tight junction protein ZO-1 by corneal endothelial cells and the density of corneal endothelial cells. We also investigated the longer-term effects of CpG-induced corneal inflammation to determine if CpG-induced corneal inflammation was associated with any detrimental effects to the corneal endothelium at later time points.

We tested the hypothesis that endothelial expression of the tight junction protein ZO-1 would be altered during experimental sterile corneal inflammation. The relationship between corneal edema, endothelial ZO-1 expression, and endothelial cell density (ECD) was also examined to determine if corneal edema was associated with a compromised endothelium.

Methods

Animals

A total of 70 female C57BL/6J mice, aged 7 to 8 weeks, were obtained from the Animal Resources Centre (Canning Vale, WA, Australia) and housed at the Florey Institute of Neuroscience and Mental Health under specific pathogen-free conditions. All animals were treated in accordance with the guidelines of the Animal Ethics Committee at the University of Melbourne, Australia, and the Florey Institute of Neuroscience and Mental Health and all animal procedures conformed to the ARVO Statement for the Use of Animals in Ophthalmic and Vision Research.

Mouse Model of Corneal Inflammation

Mice were anesthetized with an intraperitoneal injection of ketamine (80 mg/kg) and xylazine (10 mg/kg) and the epithelium of the central cornea (1 mm diameter) was debrided using an ophthalmic burr (Algerbrush II; Alger Equipment Co., Lago Vista, TX, USA), as previously described.[6] Following the central corneal abrasion, 20 μg of phosphorothioate CpG 1826 (type B, TLR-9 ligand; Invivogen, San Diego, CA, USA) or sterile saline was applied to each eye. Animals were euthanized at 24 hours, 1 week and 4 weeks after treatment by lethal injection of sodium pentobarbitone (Lethabarb; Virbac Pty Ltd., Milperra, NSW, Australia).

Spectral-Domain OCT

Mice were anesthetized and a drop of sterile saline was applied to the eye to prevent corneal drying. Mice were placed on the animal imaging mount and rodent alignment stage (AIM-RAS) attached to an SD-OCT imaging device (Bioptigen Envisu R2200 VHR; Bioptigen, Inc., Durham, NC, USA). Once the eye was aligned with the noncontact objective lens, any excess saline was absorbed using a cotton tip. Volumetric 4×4 mm rectangular scans of the anterior segment (1000 A-scans/100 B-scans) were captured using an OCT device with an 18-mm telecentric lens (Envisu R-2200; Bioptigen, NC, USA) at baseline (Figs. 1A, 1B), 24 hours, 1 week, and 4 weeks post corneal injury and topical application of CpG-ODN or saline. We analyzed OCT scans using ImageJ software (http://imagej.nih.gov/ij/; provided in the public domain by the National Institutes of Health, Bethesda, MD, USA).

Quantification of Central Corneal Thickness (CCT) From SD-OCT Scans

Total CCT was quantified, using the 4×4 mm SD-OCT images, as the distance from epithelium to endothelium at a point where a vertical line was orthogonal to the anterior-corneal curvature. Epithelial and stromal thicknesses were also quantified. A central image frame was determined, as we have previously described,[6] and CCT was taken as the mean measure from 11 frames, being the central image frame, five adjacent superior and inferior image frames.

Wholemount Immunofluorescence

Eyes were enucleated and fixed in 4% paraformaldehyde overnight at 4°C (Sigma-Aldrich Corp., Castle Hill, NSW, Australia). Corneal wedges were dissected and incubated in 20 mM EDTA at 37°C for 60 minutes, followed by blocking buffer containing 3% bovine serum albumin (BSA) and 0.3% Triton X-100. Corneas were incubated overnight in blocking buffer containing rabbit anti-ZO-1 (anti-ZO-1, 1:500; Invitrogen, Camarillo, CA, USA) primary antibody. In a subset of animals from the 4-week time point, rat anti-mouse CD45 (1:400; BD Pharmingen, San Diego, CA, USA) was included in the staining protocol. Tissues were washed with PBS and incubated in secondary goat anti-rabbit biotin (1:300; Vector Laboratories, Burlingame, CA, USA) for 3 hours followed by Streptavidin Cy3 (1:400; Jackson ImmunoResearch, West Grove, PA, USA) or goat anti-rat 488 (1:500; Invitrogen, Carlsbad, CA, USA) secondary antibody for 45 minutes. In order to visualize cell nuclei, all tissues were incubated with fluorescent dye (Hoechst, 1:500; Roche Applied Science, Mannheim, Germany) for 10 minutes at room temperature before cover slipping. Stained corneas were mounted on glass slides with the corneal epithelium facing downward.

Confocal Imaging and Quantification of ECD

To quantify the density of $CD45^+$ cells in the stroma at 4 weeks post treatment, full thickness confocal *z*-series were collected from the central cornea of a subset of animals using a ×40 objective lens; $CD45^+$ cells were counted in ImageJ. To quantify the expression of endothelial ZO-1 and ECD, two randomly selected areas of the central corneal endothelium (Fig. 1C) were imaged using a ×40 objective lens (Confocal Laser Scanning Platform SP8; Leica Microsystems, Buffalo Grove, IL, USA), representing an area of 168,200 μm^2. Corneal endothelial cells were manually counted using FIJI/Image J and converted to cells/mm^2. The relative intensity of ZO-1 expression was determined by calculating the mean number of intensity peaks exceeding a noise threshold, defined as 2-fold above average pixel intensity, using the plot profile function in ImageJ (Fig. 1D).

Image Processing and Cell Segmentation

Confocal images of ZO-1 immunostained corneas were analyzed using FIJI software.[14] Maximum intensity *z*-stacks were generated and the red channel (ZO-1) was isolated to show only the corneal endothelial cell membrane (Fig. 1E). To correct for any uneven background illumination, a pseudo flat-field correction was performed by subtracting a duplicate Gaussian blurred background ("Pseudo flat field correction") from the image. Contrast was then enhanced ("Enhance contrast") followed by binary conversion, which was performed using Li's method of thresholding ("Auto Threshold").[15] The image was further processed using a series of binary operations ("Binary…") to enhance the appearance of

Investigative Ophthalmology & Visual Science

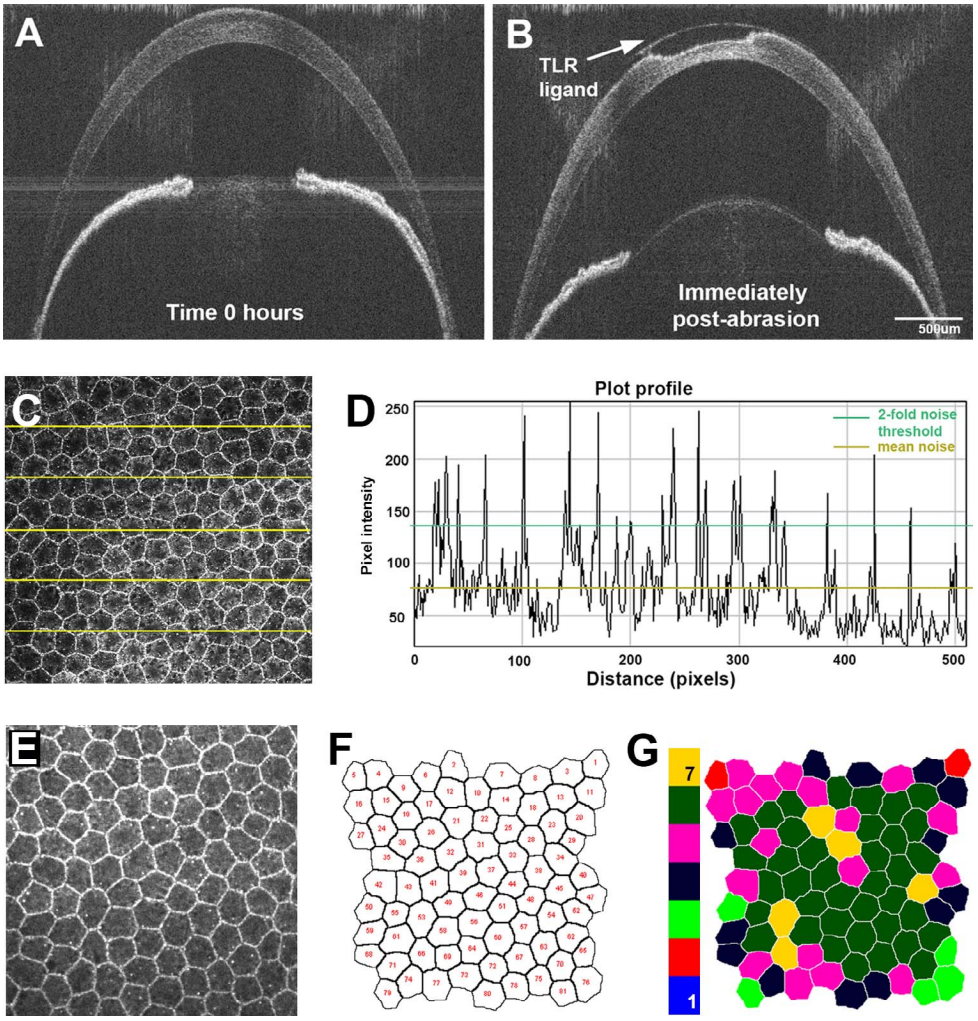

Figure 1. The methodologic approach to corneal endothelial cell analysis. (**A**) An anterior segment SD-OCT image of a C57BL/6 mouse at baseline (0 hours) and (**B**) immediately after corneal epithelial abrasion and the application of a TLR ligand to the injured region, to induce sterile corneal inflammation. (**C**) A confocal image of the central corneal endothelium, stained immunohistochemically for ZO-1. The *horizontal yellow lines* were used to derive a plot profile (**D**). To quantify corneal endothelial ZO-1 expression, the average number of peaks in the plot profile exceeding a pixel intensity threshold, defined as twice the mean background intensity (*green line*), was determined for each *horizontal line*. (**E**) The central 50% of each field was defined as an ROI and underwent image processing using a pseudo flat-field correction. (**F**) The image was further processed using a series of binary operations to enhance the appearance of the endothelial borders and allow for the creation of a skeletonized representation of the endothelial layer using a Voronoi matrix. (**G**) The degree of endothelial cell polymorphism was quantified by assessing the proportion of cells with six sides within the ROI (*green*), as a proportion of the total number of cells. The *colored* scale on the *left-hand* side indicates the number of sides for each cell.

the endothelial borders and allow for the creation of a skeletonized representation of the endothelial layer using a Voronoi matrix (Fig. 1F).

ECD and Polymegethism

The central 50% of the resultant image (205 × 205 µm) was defined as a region of interest (ROI) and analyzed using "Particle Analyzer. . ." to quantify endothelial cell number, cell area, and also the area of each endothelial cell nucleus. The degree of endothelial cell polymegethism, measured by quantifying variability in corneal endothelial cell size and nucleus size, was also analyzed. The mean cell area within the ROI was divided by the standard deviation to determine the coefficient of variation (CoV).[16] At each time point, the mean CoV of naïve (untreated) eyes was used to define a threshold value for "physiological polymegethism." The proportion of eyes with a CoV above this criterion in each group was analyzed to quantify the amount of nonphysiological corneal endothelial cell polymegethism.

Endothelial Cell Polymorphism

Images were processed as above using FIJI software with the BioVoxxel Toolbox (http://imagej.net/BioVoxxel_Toolbox; provided in the public domain by the National Institutes of Health, Bethesda, MD, USA). Hexagonality was determined by identifying cells with six adjacent neighbors using "BioVoxxel Toolbox. . .," "Neighbor Analysis" (Fig. 1G, green cells). This returned a total count of all cells present and their corresponding number of neighbors. To assess for endothelial cell polymorphism, herein defined as the degree of departure from a hexagonal cell shape, a hexagonality index was derived by dividing the number of six-sided cells by the total number of cells. A hexagonality index of 1 therefore represents all cells

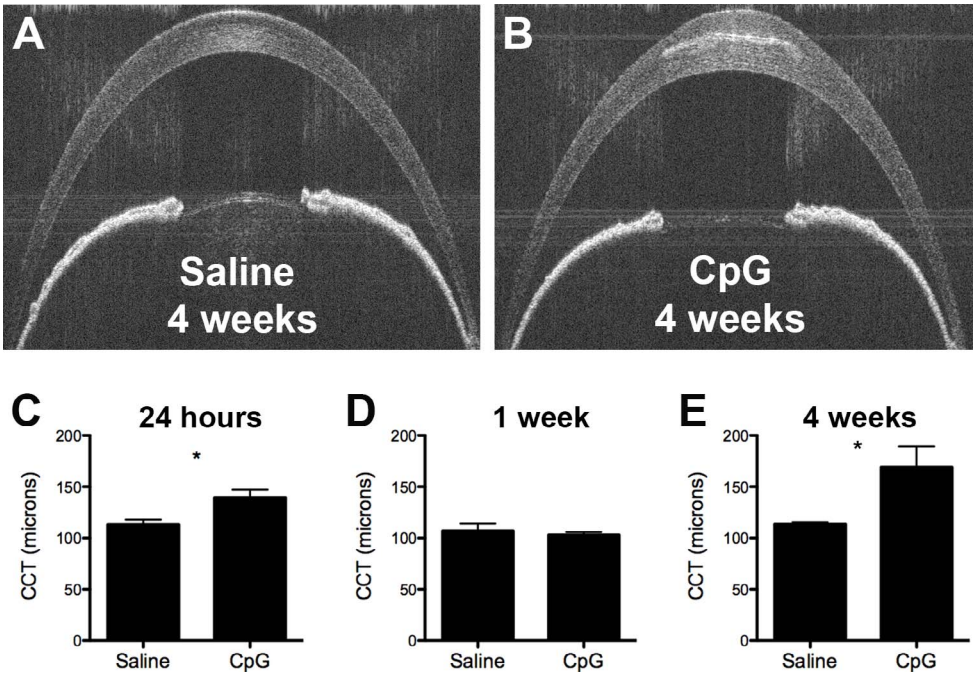

FIGURE 2. Quantification of CCT. Representative SD-OCT scans of (**A**) saline- and (**B**) CpG-ODN–treated eyes at 4 weeks post corneal injury. (**C**) Corneal thickness was increased in CpG-treated eyes at 24 hours ($P < 0.05$), but had normalized ($P > 0.05$) by 1 week (**D**). At 4 weeks post treatment, corneal thickness was again greater in CpG-ODN–treated eyes ($P < 0.05$). Data presented are mean ± SEM of six to nine mice per group. *$P < 0.05$.

were hexagonal and an index of 0 indicates none of the cells were hexagonal.

Statistical Analyses

Data were analyzed by masked observers. Descriptive statistics are summarized as mean ± SEM. Statistical analyses were performed using unpaired, 2-tailed Student's *t*-test or ANOVA (GraphPad Prism, version 6.0; GraphPad Software, Inc., La Jolla, CA, USA), followed by Bonferroni post hoc tests to determine interactions in relation to the factors of time and treatment group. Fisher's exact test was used to compare proportions. Pairwise correlations were explored using Spearman's correlation coefficient (r). An alpha of 0.05 was considered statistically significant.

RESULTS

Central Corneal Thickness

We previously reported that CpG-ODN induced corneal inflammation is associated with increased corneal thickness at 24 hours, but this subsides by 1 week.[6] In the present study, we included a later time point to examine whether the resolution of corneal edema at 1 week marked the end of the inflammatory response. Representative central anterior segment SD-OCT scans are shown 4 weeks after topical application of saline (Fig. 2A) and CpG-ODN (Fig. 2B). Relative to saline-treated eyes, mean CCT was increased in CpG-ODN–treated eyes at 24 hours post treatment (Fig. 2C, $P < 0.05$). At 1 week, there was a relative normalization of CCT in CpG-ODN–treated eyes with no significant difference between groups (Fig. 2D, $P > 0.05$). By 4 weeks, CCT was again relatively increased in CpG-ODN–treated eyes (Fig. 2E, $P < 0.05$). At 4 weeks, there was no significant difference in corneal epithelial thickness between saline- and CpG-ODN–treated eyes (33.11 ± 2.05 μm versus 52.68 ± 11.08 μm; $P = 0.11$), but stromal thickness was relatively increased in CpG-ODN–treated eyes (75.32 ± 5.33 μm versus 127.4 ± 18.27 μm; $P = 0.01$; $n = 6$ per group).

Corneal Endothelial ZO-1 Expression

Our original hypothesis was that CpG-induced corneal edema would be associated with a downregulation of ZO-1. To examine this relationship, we compared the expression intensity of ZO-1 in the corneal endothelium of CpG-treated eyes with age-matched naïve (untreated) and saline-treated eyes. Compared to naïve corneas, ZO-1 expression in the corneal endothelium was unchanged in saline-treated eyes at each of 24 hours (Figs. 3A, 3C), 1 week (Figs. 3D, 3F), and 4 weeks (Figs. 3G, 3I). In eyes treated with CpG-ODN, there was a significant reduction in corneal endothelial expression of ZO-1 at 24 hours (Figs. 3B, 3C, $P < 0.05$), which had returned to normal levels by 1 week (Figs. 3E, 3F) and then remained unchanged at 4 weeks post treatment (Figs. 3H, 3I). There was no significant difference in corneal endothelial expression of ZO-1 between saline- and CpG-ODN–treated eyes at any time point.

Corneal ECD, Polymegethism, Polymorphism, and Nucleus Size

Corneal endothelial polymegethism (measured using the CoV for cell size); polymorphism (quantified with the hexagonality index); and cell nucleus size are summarized in the Table. There was no significant difference between any groups for any of these parameters, at any of the time points. There was no difference in corneal ECD between any of the groups at 24 hours or 1 week. At 4 weeks post treatment, corneal ECD was reduced only in the CpG-ODN group, compared with naïve

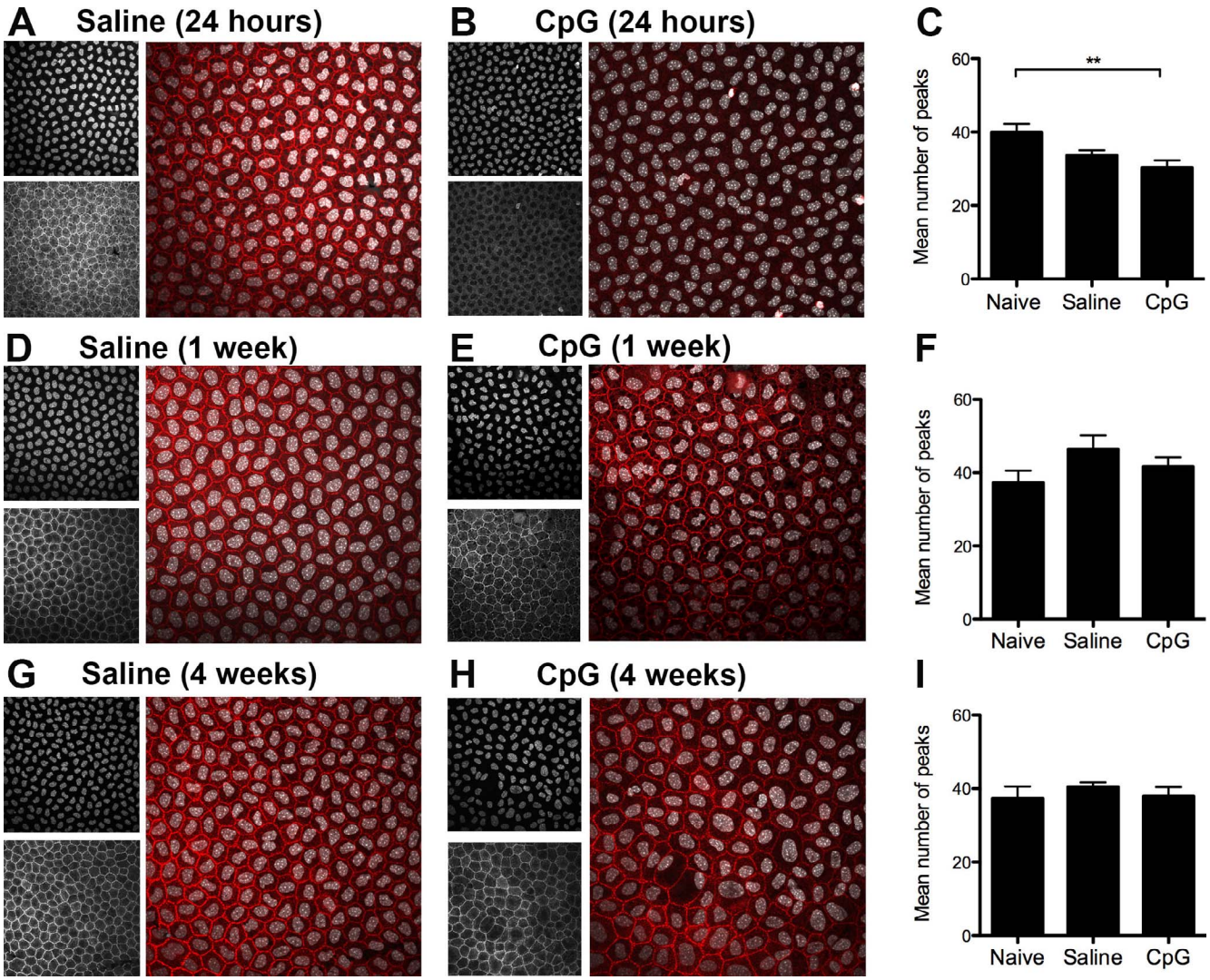

Figure 3. Corneal endothelial ZO-1 expression. Representative confocal images of the central corneal endothelium stained for ZO-1 (*red*) and cell nuclei (Hoechst, *white*) at (**A**, **B**) 24 hours, (**D**, **E**) 1 week and (**G, H**) 4 weeks post injury. (**C**) Compared with the naïve group, a reduction in ZO-1 expression was evident in CpG-treated eyes only at 24 hours ($P < 0.05$); however, this reduction was not statistically significant when compared to the saline group. This effect was attenuated by 1 week (**F**) and remained unchanged at 4 weeks (**I**). Data presented are mean ± SEM of six to nine mice per group. $^{**}P < 0.01$.

eyes (Table). There was a moderately strong, negative correlation between corneal ECD and CCT at 4 weeks (Fig. 4A, $r = -0.57$, $P = 0.02$). Plotting ECD data from all time points against CCT demonstrated a similar correlation between these parameters (Fig. 4B, $r = -0.53$, $P = 0.004$).

Despite not reaching statistical significance, we observed a slight upward trend in the CoV for endothelial cell size for CpG-ODN–treated eyes. To explore this further, we dichotomized the data to consider the proportion of eyes with a cell size CoV above the mean of naïve eyes at each time point, which was defined as the threshold for "physiological polymegethism." This value corresponds closely with other reports of normal CoV in the mouse cornea.[16] At 24 hours, only CpG-ODN eyes showed a relatively higher proportion of

Table. Corneal Endothelial Cell Density (ECD), Polymegethism (CoV), Polymorphism (hexagonality index, HEX%), and Nucleus Size

	24 Hours			1 Week			4 Weeks		
	Naïve, $n = 7$	**Saline, $n = 9$**	**CpG-ODN, $n = 10$**	**Naïve, $n = 7$**	**Saline, $n = 6$**	**CpG-ODN, $n = 11$**	**Naïve, $n = 9$**	**Saline, $n = 8$**	**CpG-ODN, $n = 8$**
ECD, μm²	2595 ± 112	2505 ± 62	2529 ± 54	2595 ± 112	2663 ± 158	2365 ± 27	2396 ± 83	2245 ± 78	2055 ± 101*
CoV	18.2 ± 1.7	19.6 ± 1.9	20.4 ± 0.9	18.2 ± 1.7	17.7 ± 1.9	19 ± 1.0	19.3 ± 1.2	22.7 ± 1.1	23.4 ± 2.2
HEX%	36 ± 1.4	36 ± 2.6	37 ± 1.0	36 ± 1.4	37 ± 1.1	36 ± 1.0	36 ± 1.7	34 ± 1.1	34 ± 1.8
Nucleus, μm²	141 ± 7	140 ± 4	135 ± 5	141 ± 7	148 ± 10	159 ± 3	148 ± 3	155 ± 2	148 ± 5

Data are shown as mean ± SEM. HEX%, percent of hexagonal cells.
* $P < 0.05$ compared with naïve eyes at the same time-point.

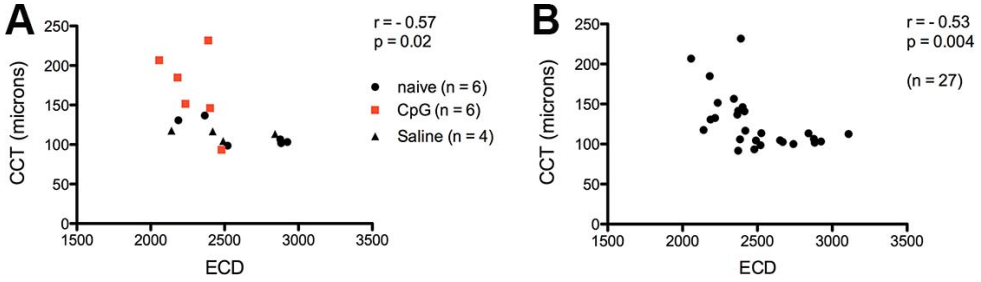

FIGURE 4. Relationship between corneal ECD and CCT. (**A**) Plot showing the relationship between ECD and CCT in naïve (*black circles*), saline-treated (*black triangles*) and CpG-treated (*red squares*) eyes at 4 weeks. There was a significant negative correlation between ECD and CCT ($r = -0.57$, $P = 0.02$). (**B**) Plot showing the relationship between ECD and CCT for all eyes at all time points. There was a significant negative correlation between ECD and CCT ($r = -0.53$, $P = 0.004$).

cells with CoVs above threshold (Fig. 5A, $P < 0.001$). At 1 week and 4 weeks, both saline- and CpG-ODN–treated eyes had a significantly higher proportion of cells with CoVs above threshold (Fig. 5A, $P < 0.001$). Using a similar approach for cell nucleus size, at 24 hours only CpG-ODN–treated eyes showed a relatively higher percentage of cells with cell CoVs above baseline threshold (Fig. 5B, $P < 0.001$). At 1 and 4 weeks, both saline- and CpG-ODN–treated eyes had a higher proportion of cells with cell nuclei size CoVs above threshold (Fig. 5B, $P < 0.001$).

Corneal Stromal Inflammatory Cells

In light of our previous reports of the presence of giant stromal macrophages and the keratic precipitates adhering to the corneal endothelium 1 week following topical CpG-ODN,[13] we examined whether the clinically observable corneal edema (Fig. 2B) and alterations to the corneal endothelium (Table) were associated with persistence of inflammatory cells in the cornea after 4 weeks. Compared with saline-treated corneas, which exhibited normal numbers of stromal leukocytes (Fig. 6A), there were elevated numbers of large $CD45^+$ cells throughout the corneal stroma (Figs. 6B, 6C) at 4 weeks post treatment ($P < 0.05$).

DISCUSSION

Experimental models of sterile TLR activation provide important insights into the nature of host inflammatory responses to particular pathogen-associated molecular patterns. Cytosine-phosphate-guanosine–DNA is a synthetic mimic of unmethylated DNA that induces transcriptional activation of proinflammatory cytokines in a TLR9-dependent manner.[17] Many studies have utilized CpG to mimic the inflammatory response that ensues during microbial infections in a range of tissues, including the lung,[18] brain,[19] and skin.[20] In the mouse cornea, CpG induces inflammation that closely parallels the immunopathology associated with herpes simplex virus type I (HSV-1) keratitis, including stromal lesions,[21] angiogenesis,[22] chemokine production[23] and activated macrophages.[13] Our laboratory, and others, have previously reported that acute corneal inflammation induced by topical CpG is associated with corneal edema, as indicated by increased CCT at 24 hours,[11] which subsides by 1 week post treatment.[6] To explore the mechanisms underlying this CpG-induced stromal edema, we investigated the expression of the tight junction protein ZO-1 and other indices of endothelial integrity including cell density, polymorphism, and polymegethism over 4 weeks.

The expression of tight junctions in the basolateral compartment of corneal endothelial cells is vital for the maintenance of deturgescence.[24] In our model of CpG-induced inflammation, ZO-1 expression was significantly reduced in the endothelium at 24 hours, when compared with naïve corneas, but this had resolved by 1 week post treatment. However, the lack of difference between the saline and CpG-treated groups suggests there is no major role for ZO-1 expression in the maintenance of corneal hydration during the acute phase of CpG-induced inflammation.

The physiological attrition of corneal endothelial cells during aging is well described in both humans[25] and mice.[26] In one study of age-related changes in the normal mouse corneal endothelium, there was a 10% decrease in ECD the ages of 6 and 16 weeks. To avoid any age-related changes impacting upon differences in ECD in our experimental groups, particularly at the 4-week time point, we included age-matched control animals. We found that treatment with the TLR-9 agonist, CpG, led to a 15% reduction in ECD compared with age-matched controls after 4 weeks. This decrease in ECD

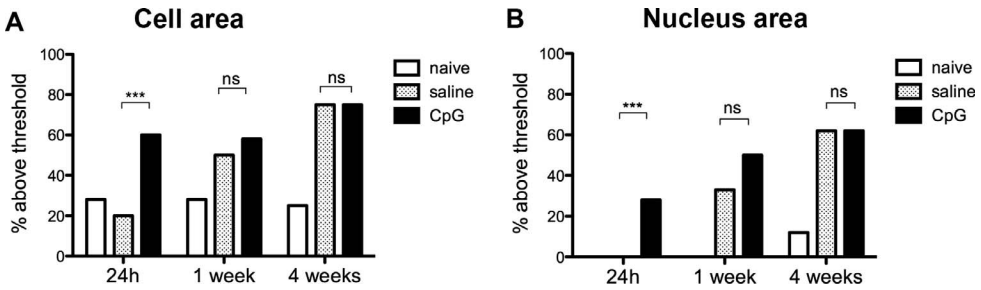

FIGURE 5. Quantification of corneal endothelial cell polymegethism and cell nucleus size. Graphs showing the proportion of eyes with a cell size CoV exceeding the mean of naïve (untreated) eyes for (**A**) polymegethism and (**B**) nucleus size. At 24 hours, only CpG-ODN eyes had a relatively higher proportion of cells with CoVs above threshold for both polymegethism and nucleus size ($P < 0.001$). At 1 and 4 weeks, both saline- and CpG-ODN–treated eyes had a higher proportion of cells with CoVs above threshold ($P < 0.001$). Data presented are mean ± SEM of six to nine mice per group. $^{**}P < 0.01$. $^{***}P < 0.001$. ns, not statistically significant; $P > 0.05$.

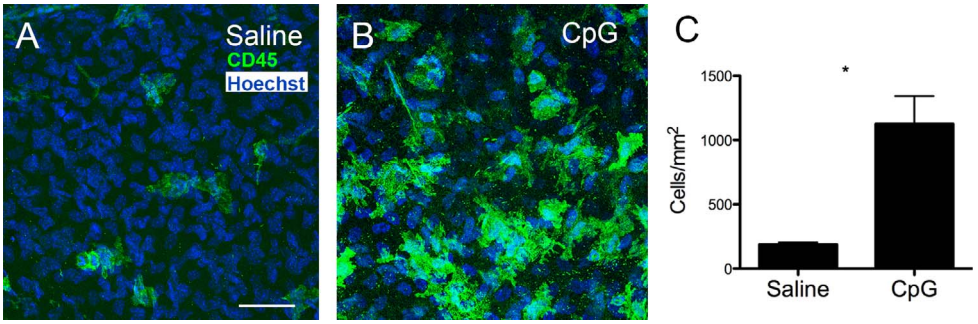

FIGURE 6. Corneal stromal inflammatory cell infiltration. Representative confocal images of the central corneal stroma stained for bone marrow-derived cells (CD45, *green*) and cell nuclei (Hoechst, *blue*) at 4 weeks post treatment. (**A**) In saline-treated eyes, CD45+ cells were evident throughout the corneal stroma. (**B**) Eyes treated with CpG-ODN showed a dense meshwork of cellular infiltration. (**C**) Quantification of the density of inflammatory cells confirmed significantly more CD45+ cells in CpG-treated eyes ($P < 0.05$). Data presented are mean ± SEM of three mice per group. $^{*}P < 0.05$. $^{**}P < 0.01$. $^{***}P < 0.001$.

was not associated with the presence of keratic precipitates, which were identifiable only at 1 week, nor altered expression of the tight junction protein, ZO-1. In a clinical study that examined endothelial cell changes in patients with HSV-1 endotheliitis, a 10% decline in ECD was reported after 1 year, despite clinical improvement in other endothelial alterations such as pseudoguttata and keratic precipitate infiltration.[1] These findings closely parallel our data, which indicate for the longer-term effects of chronic inflammation on the density of corneal endothelial cells.

In addition to the well-recognized detrimental effects of long-term contact lens wear on endothelial health, which occur mostly due to hypoxia,[27,28] the involvement of the corneal endothelium in response to epithelial or ocular surface abnormalities is gaining increasing attention. Endothelial cell density is reduced in patients with dry eye disease[29] and neurotrophic keratitis,[30] supporting a close interaction between ocular surface health and the integrity of the corneal endothelium. Our data suggest that a sterile, debridement injury to the corneal epithelium is sufficient to induce polymegethism of endothelial cells after 1 week, which persists up to 4 weeks. In the presence of CpG-ODN, endothelial polymegethism is observed after 24 hours and remains until at least 4 weeks after exposure. The observed morphologic changes in endothelial cells at 1 week are independent of the presence of keratic precipitates and activated stromal macrophages, which are a known feature of corneal inflammation in response to CpG-treatment.[13] For all conditions, the absolute degree of endothelial cell hexagonality was unchanged, supporting the concept that polymegethism is a more sensitive index of corneal endothelial responses to inflammation/injury than the degree of hexagonality (pleomorphism).[16]

We recently reported the presence of large, multinucleated giant macrophages in the mouse cornea 1 week after CpG-ODN treatment; however, this was not associated with any overt corneal endothelial dysfunction.[13] In the present study, intact ZO-1 expression, normal CCT, and normal ECD were observed in all groups at 1 week post treatment; however, there was reduced ECD and increased CCT at 4 weeks after CpG-ODN treatment. These signs of corneal pathology in the CpG-ODN–treated group were associated with the presence of enlarged $CD45^{+}$ cells throughout the corneal stroma, indicating persistent activation of inflammatory cells. Elevated numbers of leukocytes in the corneal stroma are a feature of chronic inflammatory processes such as allograft rejection,[31] herpetic stromal keratitis,[32] and trauma-induced neovascularization.[33] A recent study on the pathologic capacity of activated monocyte-derived cells during allograft rejection provides evidence that macrophage-derived cytokines, including interferon-γ, can directly induce corneal endothelial cell death in vitro.[34] Thus, it is possible that the persistence of activated leukocytes in our model of CpG-ODN–induced corneal inflammation contributes to the observed decline in endothelial cell density and the increased corneal thickness at 4 weeks post treatment.

Our data demonstrate that CpG-ODN–induced corneal inflammation is associated with reduced endothelial density, increased corneal thickness, and presence of activated leukocytes 4 weeks after topical treatment in mice. These chronic signs of inflammation occur independently of alterations to the expression of tight junction protein zonula occludens-1. The use of topically applied toll-like receptor-9 agonists to the injured mouse epithelium provides a model to investigate the interplay between chronic stromal leukocyte activation, corneal edema, and endothelial integrity during sterile corneal inflammation.

Acknowledgments

The authors would like to thank the Florey Advanced Microscopy Facility at The Florey Institute of Neuroscience & Mental Health Facility for provision of instrumentation, training, and general support; the following postgraduate students enrolled in the University of Melbourne Doctor of Optometry program, who contributed to initial image analysis (ZO-1 pixel intensity and endothelial cell density): Joanna Del Rosario, Kahla Best, Danielle Di Pasquale, Nikhil Chinta, and Geoffrey Demare; and Jan Brocher for his contribution in the development of some of the image processing protocols used in this study.

Supported by a National Health and Medical Research Council of Australia Project Grant (HRC #1042612).

Disclosure: **L.E. Downie**, None; **J. Choi**, None; **J.K.H. Lim**, None; **H.R. Chinnery**, None

References

1. Hillenaar T, Weenen C, Wubbels RJ, Remeijer L. Endothelial involvement in herpes simplex virus keratitis: an in vivo confocal microscopy study. *Ophthalmology*. 2009;116:2077–2086.
2. Trinh L, Brignole-Baudouin F, Labbé A, Raphaël M, Bourges JL, Baudouin C. The corneal endothelium in an endotoxin-induced uveitis model: correlation between in vivo confocal microscopy and immunohistochemistry. *Mol Vis*. 2008;14:1149–1156.
3. Hegde S, Beauregard C, Mayhew E, Niederkorn JY. CD4(+) T-cell-mediated mechanisms of corneal allograft rejection: role of Fas-induced apoptosis. *Transplantation*. 2005;79:23–31.

4. Steger B, Speicher L, Philipp W, Bechrakis NE. In vivo confocal microscopic characterisation of the cornea in chronic graft-versus-host disease related severe dry eye disease. *Br J Ophthalmol*. 2015;99:160–165.
5. Patel DV, McGhee CN. Quantitative analysis of in vivo confocal microscopy images: a review. *Surv Ophthalmol*. 2013;58:466–475.
6. Downie LE, Stainer MJ, Chinnery HR. Monitoring of strain-dependent responsiveness to TLR activation in the mouse anterior segment using SD-OCT. *Invest Ophthalmol Vis Sci*. 2014;55:8189–8199.
7. Srinivas SP. Dynamic regulation of barrier integrity of the corneal endothelium. *Optom Vis Sci*. 2010;87:E239–E254.
8. Yanai R, Ko JA, Morishige N, Chikama T, Ichijima H, Nishida T. Disruption of zonula occludens-1 localization in the rabbit corneal epithelium by contact lens-induced hypoxia. *Invest Ophthalmol Vis Sci*. 2009;50:4605–4610.
9. Shivanna M, Rajashekhar G, Srinivas SP. Barrier dysfunction of the corneal endothelium in response to TNF-alpha: role of p38 MAP kinase. *Invest Ophthalmol Vis Sci*. 2010;51:1575–1582.
10. Rajashekhar G, Shivanna M, Kompella UB, Wang Y, Srinivas SP. Role of MMP-9 in the breakdown of barrier integrity of the corneal endothelium in response to TNF-alpha. *Exp Eye Res*. 2014;122:77–85.
11. Johnson AC, Heinzel FP, Diaconu E, et al. Activation of toll-like receptor (TLR)2, TLR4, and TLR9 in the mammalian cornea induces MyD88-dependent corneal inflammation. *Invest Ophthalmol Vis Sci*. 2005;46:589–595.
12. Chinnery HR, McLenachan S, Binz N, et al. TLR9 Ligand CpG-ODN applied to the injured mouse cornea elicits retinal inflammation. *Am J Pathol*. 2012;180:209–220.
13. Chinnery HR, Leong CM, Chen W, Forrester JV, McMenamin PG. TLR9 and TLR7/8 activation induces formation of keratic precipitates and giant macrophages in the mouse cornea. *J Leukoc Biol*. 2015;97:103–110.
14. Schindelin J, Arganda-Carreras I, Frise E, et al. FIJI: an open-source platform for biological-image analysis. *Nature Methods*. 2012;9:676–682.
15. Li CH, Tam PKS. An iterative algorithm for minimum cross entropy thresholding. *Pattern Recogn Lett*. 1998;19:771–776.
16. Chauhan SK, Jurkunas U, Funaki T, Dastjerdi M, Dana R. Quantification of allospecific and nonspecific corneal endothelial cell damage after corneal transplantation. *Eye (Lond)*. 2015;29:136–144.
17. Hemmi H, Takeuchi O, Kawai T, et al. A toll-like receptor recognizes bacterial DNA. *Nature*. 2000;408:740–745.
18. Knuefermann P, Baumgarten G, Koch A, et al. CpG oligonucleotide activates toll-like receptor 9 and causes lung inflammation in vivo. *Respir Res*. 2007;8:72.
19. Deng GM, Liu ZQ, Tarkowski A. Intracisternally localized bacterial DNA containing CpG motifs induces meningitis. *J Immunol*. 2001;167:4616–4626.
20. Mathes AL, Rice L, Affandi AJ, et al. CpGB DNA activates dermal macrophages and specifically recruits inflammatory monocytes into the skin. *Exp Dermatol*. 2015;24:133–139.
21. Sarangi PP, Kim B, Kurt-Jones E, Rouse BT. Innate recognition network driving herpes simplex virus-induced corneal immunopathology: role of the toll pathway in early inflammatory events in stromal keratitis. *J Virol*. 2007;81:11128–11138.
22. Zheng M, Klinman DM, Gierynska M, Rouse BT. DNA containing CpG motifs induces angiogenesis. *Proc Natl Acad Sci U S A*. 2002;99:8944–8949.
23. Wuest T, Austin BA, Uematsu S, Thapa M, Akira S, Carr DJ. Intact TRL 9 and type I interferon signaling pathways are required to augment HSV-1 induced corneal CXCL9 and CXCL10. *J Neuroimmunol*. 2006;179:46–52.
24. Mandell KJ, Holley GP, Parkos CA, Edelhauser HF. Antibody blockade of junctional adhesion molecule-A in rabbit corneal endothelial tight junctions produces corneal swelling. *Invest Ophthalmol Vis Sci*. 2006;47:2408–2416.
25. Yee RW, Matsuda M, Schultz RO, Edelhauser HF. Changes in the normal corneal endothelial cellular pattern as a function of age. *Curr Eye Res*. 1985;4: 671–678.
26. Jun AS, Chakravarti S, Edelhauser HF, Kimos M. Aging changes of mouse corneal endothelium and Descemet's membrane. *Exp Eye Res*. 2006;83:890–896.
27. Holden BA, Sweeney DF, Vannas A, Nilsson KT, Efron N. Effects of long-term extended contact lens wear on the human cornea. *Invest Ophthalmol Vis Sci*. 1985;26:1489–1501.
28. Bonanno JA. Effects of contact lens-induced hypoxia on the physiology of the corneal endothelium. *Optom Vis Sci*. 2001; 78:783–790.
29. Kheirkhah A, Saboo US, Abud TB, et al. Reduced corneal endothelial cell density in patients with dry eye disease. *Am J Ophthalmol*. 2015;159:1022–1026.e2.
30. Lambiase A, Sacchetti M, Mastropasqua A, Bonini S. Corneal changes in neurosurgically induced neurotrophic keratitis. *JAMA Ophthalmol*. 2013;131:1547–1553.
31. Larkin DF, Alexander RA, Cree IA. Infiltrating inflammatory cell phenotypes and apoptosis in rejected human corneal allografts. *Eye (Lond)*. 1997;11(pt 1):68–74.
32. Bauer D, Mrzyk S, van Rooijen N, Steuhl KP, Heiligenhaus A. Macrophage-depletion influences the course of murine HSV-1 keratitis. *Curr Eye Res*. 2000;20:45–53.
33. Sonoda KH, Nakao S, Nakamura T, et al. Cellular events in the normal and inflamed cornea. *Cornea*. 2005;24:S50–S54.
34. Lapp T, Zaher SS, Haas CT, et al. Identification of therapeutic targets of inflammatory monocyte recruitment to modulate the allogeneic injury to donor cornea. *Invest Ophthalmol Vis Sci*. 2015;56:7250–7259.

Investigative Ophthalmology & Visual Science